RSC Advances

ROYAL SOCIETY OF CHEMISTRY

www.rsc.org/advances

Cite this: DOI: 10.1039/c0xx00000x

www.rsc.org/xxxxxx

ARTICLE TYPE

Triphenylphosphine modified graphene quantum dots: spectral modulation for full spectrum of visible light with high quantum yield

Siwei Yang [a†], Chong Zhu[a, b†], Jing Sun [a], Peng He [a], Ningyi Yuan [b], Jianning Ding [b], Guqiao Ding [a*], Xiaoming Xie [a]

Received (in XXX, XXX) Xth XXXXXXXXX 20XX, Accepted Xth XXXXXXXXX 20XX
DOI: 10.1039/b000000x

We report the triphenylphosphine ($P(Ph)_3$) modified graphene quantum dots (P-GQDs) with high quantum yield (*c*) and excellent stability. The light energy absorbed by $P(Ph)_3$ groups can fast and efficiently transfer to the GQDs through the C-P-$(Ph)_3$ bonds, resulting in a high φ. The obtained P-GQDs have tunable photoluminescence wavelength from blue to red, and at the same time maintain a high φ over 58%, with the increasing of permittivity of the solvents. The main mechanism of full-visible-light-specrtrum modulation can be due to the energy loss and electron-donating decrease caused by $P(Ph)_3$ group-solvent interaction or relaxation.

Graphene quantum dots (GQDs) is a rising star in the family of fluorescent materials. [1-5] GQDs have superior properties, such as high photostability, biocompatibility, and low toxicity compared with organic dyes [6-7] and semiconductor quantum dots [8-14]. Moreover, GQDs clearly contain a 2D graphene structure regardless of the dot size and shape, which is different with hydrothermally synthesized carbon dots. [15-17] However, there are still some demanding challenges in practical applications of GQDs, such as low quantum yield (φ) and controllable spectral modulation. [1-3, 18] The low φ means low fluorescent intensity. So far, most reported GQDs just have a φ lower than 0.5, [19-20] and almost all reported GQDs absorb and emit relatively short wavelength light (maximum emission wavelengths λ_{em}＜500 nm), as detailedly listed in Table S1. The GQDs with short emission wavelength have poor tissue permeability, and may cause photodamages to the tissue, and are easily interfered by biological self fluorescence. [2-4, 18, 21] It is clear that, both the low φ and short λ_{em} restrict the applications of GQDs in fluorescent bio-imaging, light harvesters, sensitizers for photodynamic therapy and solar cells.

By now, mainstream technologies for spectral modulation and photoluminescence enhancing of GQDs are based on doping and modification (Table S1). We reported the 1-3 nm nitrogen doped GQDs with the highest quantum yield of 0.74 via cutting graphene oxide precursor and in-situ lattice doping progress without further surface passivation or modification. [18] Lee *et al.* reported the synthesis of near infra-red GQDs and their biological application for optical imaging of deep tissues and organs. [22] However, there are few reports about the synthesis of GQDs with both tunable spectrum and high quantum yield at the same time. It is well know that GQDs have excitation wavelength dependent emission, i.e., the λ_{em} varies with different excitation wavelenghth. Generally, the quantum yiled with most excitation wavelenghths is very low. [18-22]

Here, we report the triphenylphosphine ($P(Ph)_3$) modified GQDs (P-GQDs) with high quantum yield over 58% among the full visible light range from blue to red. The $P(Ph)_3$ groups on P-GQDs absorb light energy, which can fast and efficiently transfer to the GQD fluorophores through the C-P-$(Ph)_3$ bondings, resulting in a high quantum yield. The λ_{em} of P-GQDs red shifted from 431 to 641 nm with the increasing of dielectric constant (ε) of solvents. The spectral modulation mechanism is proposed and discussed.

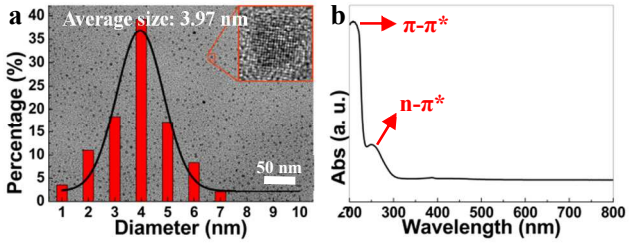

Fig. 1 (a) TEM image and corresponding size distribution histogram of P-GQDs, the black line is the Gaussian fitting curve. Inset: RTEM image of a single P-GQDs particle. (b) UV-vis absorption spectrum of P-GQDs aqueous solution.

The P-GQDs were prepared as follows: typically, 2.0 mL 100 mM triphenylphosphine DMF solution was added to 8.0 mL, 1 mg mL^{-1} graphene oxide quantum dots (GOQDs) DMF solution, and then the mixture was transferred into a 15 mL Teflon®-lined autoclave and heated and kept at 260 °C for 72 h. After that, the mixture was filtered using an alumina inorganic membrane with 20 nm pores. The resulting filtrate diluted with water and was dialysed in a 500 Da dialysis bag against deionised water for a week to remove excess salt. The P-GQD yield from GOQDs is approximately 61%.

As shown in Figure 1 a, the P-GQDs exhibited excellent uniformity. The average diameter of P-GQDs is 3.97 and the size distribution accords well with Gaussian distribution. The full-

widthat-half-maximum (FWHM) of the fitted Gaussian curve is 1.42 nm, indicating the narrow distribution nature of the P-GQDs. The size distribution exhibits no obvious change after doping (Fig. S1). The high-resolution TEM image, as shown in Fig. 1a inset reveals the high crystallinity of the P-GQDs showing the crystallinity with lattices of 0.226 nm. [2, 18, 23] This can be attributed to the (002) facet of graphitic carbon.[18]

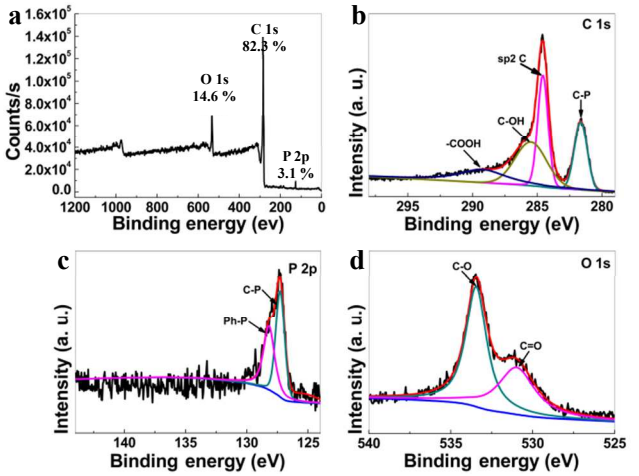

Fig. 2 (a) XPS survey spectrum of P-GQDs. (b) C1s XPS spectrum, (c) P 2p XPS spectrum, (d) O1s XPS spectrum of P-GQDs.

The UV-vis spectrum of P-GQD solution (Figure 1b) shows an absorption peak at 209 nm, which is ascribed to the π-π* transition of C=C in conjugated structure. The significant absorption peak at ca. 250 nm reveals the n-π* transition of p-π orbit between the P and conjugate structure. [24-25] The XPS survey spectrum of P-GQDs is shown in Fig. 2a, showing a narrow graphitic C 1s peak at ca. 284.2 eV, a O 1s peak at ca. 532 eV an a P 2p peak at ca. 126 eV. Fig. 1b shows the well-fitted C1s spectrum, which can be divided into four different peaks, corresponding to the signals of C-C and C=C (284.6 eV), C-OH (285.4 eV), -COOH (289.1 eV) and C-P (281.6 eV). [24-26] The P 2p spectrum can be divided into two different peaks (Fig. 1c), corresponding to the signals of P-C (127.3 eV) and P-Ph (128.2 eV). Moreover, the O 1s spectrum also can be divided into two different peaks (Fig. 2d), which correspond to the signals of C-O (533.5 eV) and C=O (531.0 eV). [27] Thus, the $P(Ph)_3$ have been successfully used to modify the GQD via the C-P-$(Ph)_3$ bonding mode. [25] The FT-IR spectrum of P-GQDs is shown in Fig. S2. The adsorption peaks at 3500-2500 cm^{-1} corresponding to the -OH stretching mode, which implying the presence of -OH and -COOH. The peak at 1790 cm^{-1} can be attributed to the stretching vibration of C=O. The strong absorption peak at 1150 cm^{-1} can be due to the stretching vibration of P-Ar groups. The peak at 950 cm^{-1} can be attributed to the stretching vibration of C-O-C. Moreover, the bands at 754 and 593 cm^{-1}, characteristic of C-H out-of-plane bending vibrations of benzene nuclei in the benzene ring.

The optical properties are shown in Fig. 3. The P-GQDs DMF solution exhibited maximum excitation (λ_{ex}) and emission (λ_{em}) wavelengths at 460 and 532 nm, respectively (Fig. 3a). The optical images indicate the P-GQDs giving bright blue-green photoluminescence (PL) under UV light (Fig. 3a inset). The Stokes shift ($\Delta\nu_{St}$) and FWHM of P-GQDs are 0.36 eV and 0.24 eV, respectively. The low $\Delta\nu_{St}$ indicates that the P-GQDs have a weak self-absorption effect and low energy loss. The φ of P-GQDs is 0.64, which is higher than most previous reports (Table S1). [1-6, 18, 28]

The PL decay of P-GQDs is measured by a time-correlated single photon counting technique, and fitted well with a bi-exponential decay as shown in Fig. 3b. The lifetime (τ) is dominated by a long decay component of 7.1 ns (88%) plus a small contribution from the short decay of 1.3 ns (12%): the weighted-average lifetime is approximately 6.4 ns. However, the physics of fast and slow decay in GQDs is unclear which can be due to the complex PL mechanism and diverse surface activity groups. Combining the φ and τ by $\kappa_r = \varphi/\tau$, we can obtain the radiative rates κ_r. [24] The fluorescence radiative rate κ_r of P-GQDs is 1.0×10^8 s^{-1}. [30-32]

The P-GQDs exhibit a maximum emission wavelength shift of 26 nm when the excitation wavelength increases from 410 to 500 nm. Moreover, the P-GQDs showed excellent photostability under UV light (Fig. 3d). The PL intensity have no obvious cha nge under 150 W Xe lamp with centre wavelength at 320 nm for 24 h. Moreover, the PL intensity of P-GQDs is also stable when the pH value was changed from 1 to 14 (Fig. S3). The good stability is due to the pH insensitive groups P-$(Ph)_3$ on P-GQDs.

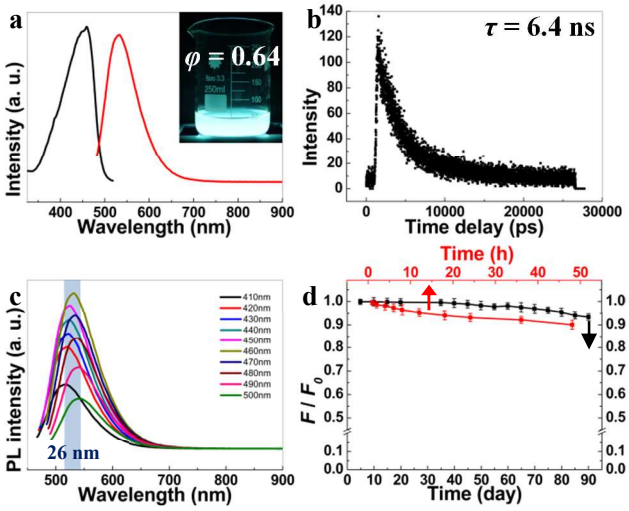

Fig. 3 (a) Normalized PLE (black curve) and PL (red curve) spectra of P-GQDs DMF solution. Inset: digital image of P-GQDs DMF solution under UV-light (centre wavelength: 365 nm). (b) PL decay curves of P-GQDs measured at room temperature and excitations at 460 nm. (c) PL spectra of P-GQDs with different excitation wavelength (410, 420, 430, 440, 450, 460, 470, 480, 490, 500 nm). (d) Photostability (red curve) of P-GQDs under UV light (150 W Xe lamp with centre wavelength at 320 nm). F_0 and F are PL intensities in 0 h and specify time, respectively.

It is interesting that the λ_{em} shifted when the P-GQDs dispersed in different solvents. Fig. 4a shows the normalized PL spectra of P-GQDs in different solvents (ethyl acetate (EA), acetone (DMK), ethanol (EtOH) , DMF, nitromethane, DMSO and water). The λ_{em} shifted from 431 to 641 nm. The the tunable optical spectrum almost covered the full spectrum of visible light (400-700 nm). The P-GQDs giving colorful bright luminescence from blue to red when P-GQDs dispersed in different solvents (Fig. 4b). Moreover, the quantum yield always kept in 0.58 or higher (red curve in Fig. 4c), which indicates the P-GQDs have good PL properties in different solution environment. Futher analyses

show that the λ_{em} is related to the permittivity (ε) of the solvents (Fig. 4c). With the increasing of ε, the λ_{em} red shifted.

The possible mechanism of the spectral modulation is shown in Fig. 4d. As a large 2D conjugated molecular structure, GQDs can be regarded as macromolecules. The photoluminescence process of GQDs is much more like that of fluorescent dyes. P-GQDs possess electron-donating ($P(Ph)_3$) groups conjugated to an electron-withdrawing 2D macromolecules (GQDs). The $P(Ph)_3$ groups have high UV absorption cross sections, [33-34] and the harvested energy can fast and efficiently transfer to the GQD fluorophores through the C-P-$(Ph)_3$ bondings. This energy transfer process affords high quantum yield, and this PL enhancement mechnism is similar to the n-π* transition between the N in aromatic ring and the conjugate structure of graphene in N-doped GQDs with very high quantum yield. [18] On the other hand, the $P(Ph)_3$ groups will be affected by the solvents due to its spatial pyramidal structure with a chiral propeller-like arrangement of the three phenyl rings. When the solvent polarity increases, the $P(Ph)_3$-solvent interaction/relaxation may lead to energy loss and decrease of the electron-donating capacity, which contributes to the red shift of the fluorescence spectra, as shown in Fig. 4b and 4c. It should be mentioned that the solvent polarity has less impact on GQDs since it has much larger 2D structure compared with $P(Ph)_3$. The energy diagram of P-GQDs with different ε is proposed in Fig. S4 for better understanding the mechanisms.

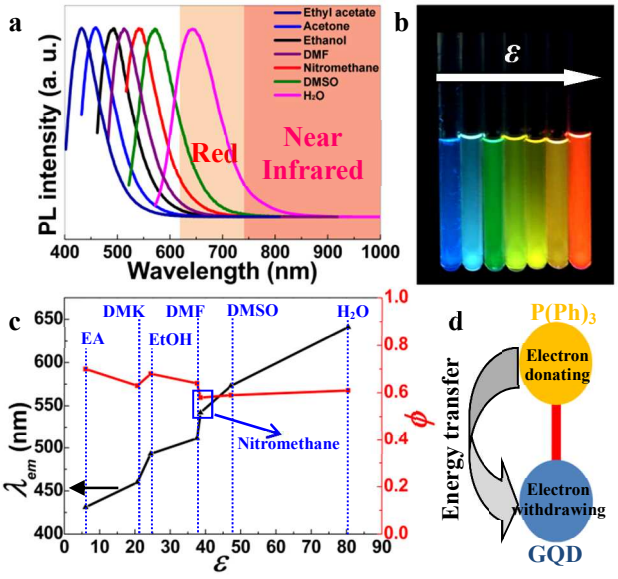

Fig. 4 (a) PL spectra of P-GQDs in different solvents. (b) Digital image of P-GQDs in different solvents under UV-light (centre wavelength: 365 nm). (c) The relation between λ_{em}, φ and ε. (d) Schematic diagram illustrating the possible mechanism of the modulation progress.

In summary, we fabricated P-GQDs with tunable spectrum from 431 to 641 nm, high quantum yield over 0.58 and exclellent stability. The $P(Ph)_3$ was connected to GQDs through the chemical C-P-$(Ph)_3$ bondings. The $P(Ph)_3$ groups absorb light energy and transfer energy to the GQDs, resulting in a high quantum yield. The energy loss and electron-donating capacity reduction due to the $P(Ph)_3$-solvent interaction/relaxation may contribute to the specrtral modulation. This work will be helpful for synthesizing new bio-imaging materials with both high quantum yield and tunable PL properties at the same time.

Acknowledgements

This work was supported by projects from the National Science and Technology Major Project (Grant no. 2011ZX02707), the Chinese Academy of Sciences (Grant no. KGZD-EW-303 and XDA02040000).

Notes and references

[a] *State Key Laboratory of Functional Materials for Informatics, Shanghai Institute of Microsystem and Information Technology, Chinese Academy of Science, Shanghai 20050, P. R. China*
[b] *School of Materials Science and Engineering, Changzhou University, Changzhou 21300, P. R. China*
†*These authors are co-first authors*
**Corresponding author: Prof. Guqiao Ding, gqding@mail.sim.ac.cn*

References

1 L. A. Ponomarenko, F. Schedin, M. I. Katsnelson, R. Yang, E. W. Hill, K. S. Novoselov, A. K. Geiml, *Science*, 2008, **320**, 356.
2 J. C. Ge, M. H. Lan, B. J. Zhou, W. R. Liu, L. Guo, H. Wang, Q. Y. Jia, G. L. Niu, X. Huang, H. Y. Zhou, X. M. Meng, P. F. Wang, C. S. Lee, W. J. Zhang, X. D. Han, *Nat. Commun.*, 2014, **5**, 4596.
3 M. Nurunnabi, Z. Khatun, K. M. Huh, S. Y. Park, D. Y. Lee, K. J. Cho, Y. Lee, *ACS Nano*, 2013, **7**, 6858.
4 L. L. Fan, M. Zhu, X. Lee, *Part. Part. Syst. Charact.*, 2013, **30**, 764.
5 M. Bacon, S. J. Bradley, N. Thomas, *Part. Part. Syst. Charact.*, 2014, **31**, 415.
6 R. Gokhale, P. Singh, *Part. Part. Syst. Charact.*, 2014, **31**, 433.
7 Y. Q. Dai, H. Long, X. T. Wang, *Part. Part. Syst. Charact.*, 2014, **31**, 580.
8 I. L. Medintz, H. T. Uyeda, E. R. Goldman, H. Mattoussi, *Nat. Mater.*, 2005, **4**, 435.
9 S. Gupta, Z. Olga, V. Aleksand, *Part. Part. Syst. Charact.*, 2013, **30**, 346.
10 L. B.Tang, R. B. Ji, X. M. Li, *Part. Part. Syst. Charact.*, 2013, **30**, 523.
11 N. Chen, Y. He, Y. Y. Su, X. M. Li, Q. Huang, H. F. Wang, X. Z. Zhang, R. Z. Tai, C. H. Fan, *Biomaterials.*, 2012, **33**, 1238.
12 B. M. Serene, H. Lara, *Part. Part. Syst. Charact.*, 2013, **30**, 706.
13 J. Xu, S. H. Sun, Y. Q. Cao, *Part. Part. Syst. Charact.*, 2014, **31**, 459.
14 S. J. Stefan, B. B. Manshian, A. Abdelmonem, *Part. Part. Syst. Charact.*, 2014, **31**, 794-800
15 W. Zhou, Z. Wang, P. He, G. Ding, X. Xie, Z. Kang, M. Jiang, *J. Mater. Chem. A*, 2014, **2**, 8660.
16 X. H. Zhu, H. Y. Wang, Q. Y. Jiao, *Part. Part. Syst. Charact.*, 2014, **31**, 771.
17 H. T. Li, X. D. He, Z. H. Kang, H. Huang, Y. Liu, J. L. Liu, S. Y. Lian, C. H. Tang, X. B. Yang, S. T. Lee, *Angew. Chem. Int. Ed.*, 2010, **49**, 4430.
18 J. Sun, S. Yang, Z. Wang, H. Shen, T. Xu, L. Sun, H. Li, W. Chen, X. Jiang, G. Ding, Z. Kang, X. Xie, M. Jiang, *Part. Part. Syst. Charact.*, DOI: 10.1002/ppsc.201400189
19 L. Zhou, J. L. Geng, B. Liu, *Part. Part. Syst. Charact.*, 2013, **30**, 1086.
20 C. K. Chang, K. Satender, C. C. Kuo, G. Abhijit, B. Y. Wang, J. Y. Hwang, K. J. Huang, W. H. Yang, S. B. Wang, C. H. Chuang, M. Chen, C. I. Huang, W. F. Pong, K. J. Song, S. J. Chang, J. H. Guo, Y. A. Tai, T. Masahiko, I. Seiji, C. W. Chen, L. C. Chen, K. H. Chen, *ACS Nano*, 2013, **7**, 1333.
21 F. Liu, M. H. Jang, H. D. Ha, H. K. Je, H. C. Yong, S. S. Tae, *Adv. Mater.*, 2013, **25**, 3657.
22 M. D. Nurunnabi, K. Zehedina, R. R. Gerald, D. Y. Lee, Y. K. Lee, *Chem. Commun.*, 2013, **49**, 5079.

23 Y. Li, Y. Zhao, H. Cheng, Y. Hu, G. Shi, L. Dai, L. Qu, *J. Am. Chem. Soc.*, 2012, **134**, 15.

24 F. Liao, S. Yang, X. Li, L. Yang, Z. Xie, C. Hu, S. Yan, T. Ren, Z. Liu, *Synth. Met*., 2014, **189**, 126.

25 F. Liao, S. Yang, X. Li, L. Yang, Z. Xie, C. Hu, L. He, X. Kang, X. Song, T. Ren, *Synth. Met.*, 2014, **189**, 135.

26 X. Song, S. Yang, L. He, S. Yan, F. Liao, *RSC Adv.*, 2014, **4**, 49000.

27 S. Yang, C. Ye, X. Song, L. He, F. Liao, *RSC Adv.*, 2014, **4**, 54810.

28 K. Lingam, R. Podila, H. Qian, S. Serkiz, A. M. Rao, *Adv. Funct. Mater.*, 2013, **23**, 5062.

29 C. Thivierge, A. Loudet, K. Burgess, *Macromolecules*, 2011, **44**, 4012.

30 S. Yang, J. Sun, X. Li, W. Zhou, Z. Wang, P. He, G. Ding, X. Xie, Z. Kang, M. Jiang, *J. Mater. Chem. A*, 2014, **2**, 8660.

31 S. Yan, S. Yang, L. He, C. Ye, X. Song, F. Liao, *Synth. Met.*, 2014, **198**, 142.

32 S. W. Yang, S. Q. S. Huang, D. Liu, F. Liao, *Synth. Met.*, 2012, **162**, 2228.

33 J.-Y. Liu, H.-S. Yeung, W. Xu, X. Li, D. K. P. Ng, *Org. Lett.*, 2008, **10**, 5421.

34 R. Hu, E. Lager, A. A. Aguilar, J. Liu, J. W. Y. Lam, H. H. Y. Sung, I. D. Williams, Y. Zhong, K. S. Wong, E. P. Cabrera, B. Z. Tang, *J. Phys. Chem. C*, 2009, **113**, 15845.